# SIMULATION OF THE PERFORMANCE OF THE LICAS TRAIN

*R. Bingham, J. Green, G. Grzelak, A. Mitra, C. Perry, A. Reichold*
*University of Oxford, UK*

## 1 INTRODUCTION

The proposed LiCAS[1] metrology system is a novel instrument dedicated to align and monitor the mechanical stability of a future linear high energy $e^+e^-$ collider. LiCAS uses Laser Straightness Monitors (LSM) and Frequency Scanning Interferometry (FSI) [1, 2][2] for straightness and distance measurements, respectively. This paper describes detailed simulations of a LiCAS system operating inside a Rapid Tunnel Reference Surveyor (RTRS train, fig. 1) [3] for a future linear collider. The measurement accuracy for a single train stop as well as the train performance over a $90\,m$ tunnel section is presented. Results obtained from the full simulation of the train are compared to a specialised random walk model of error propagation which is also used to extrapolate the expected precision over $600\,m$ tunnel section. First attempt to develop a calibration procedure for this instrument is also presented. With the proposed design it is feasible to achieve the required vertical accuracy of the order of $\mathcal{O}(200)\,\mu m$ over $600\,m$ tunnel sections meeting the specification for the TESLA collider [4].

## 2 PRINCIPLE OF THE LICAS TRAIN OPERATION

In figure 2 the schematic view of the LiCAS train operating in the accelerator tunnel is presented. The train is composed of 6 cars, the distance between the centres of neighbouring cars is $\sim 4.5\,m$. Each car is equipped with 4 CCD cameras and two beam splitters (BS) constituting the straightness monitor (fig. 3). The straightness monitor measures the transverse translation $(T_x, T_y)$ and transverse rotation $(R_x, R_y)$ with respect to a $z$ axis defined by the laser beam passing through all cars in a vacuum pipe. The laser beam is reflected back using the retro-reflector (RR) located in the last car, illuminating the upper CCD cameras of the straightness monitors. 6 FSI lines placed in the same vacuum pipe between each pair of cars are responsible for the distance measurement along the $z$ axis $(T_z)$. In addition a clinometer located on each car provides a measurement of rotation around the $z$ axis $(R_z)$. A clinometer cannot be used to determine rotation around $x$ axis as this would make the

[1]Linear Collider Alignment and Survey: R&D group at the University of Oxford.
[2]Frequency Scanning Interferometry allows for a optical measurement of absolute distances.

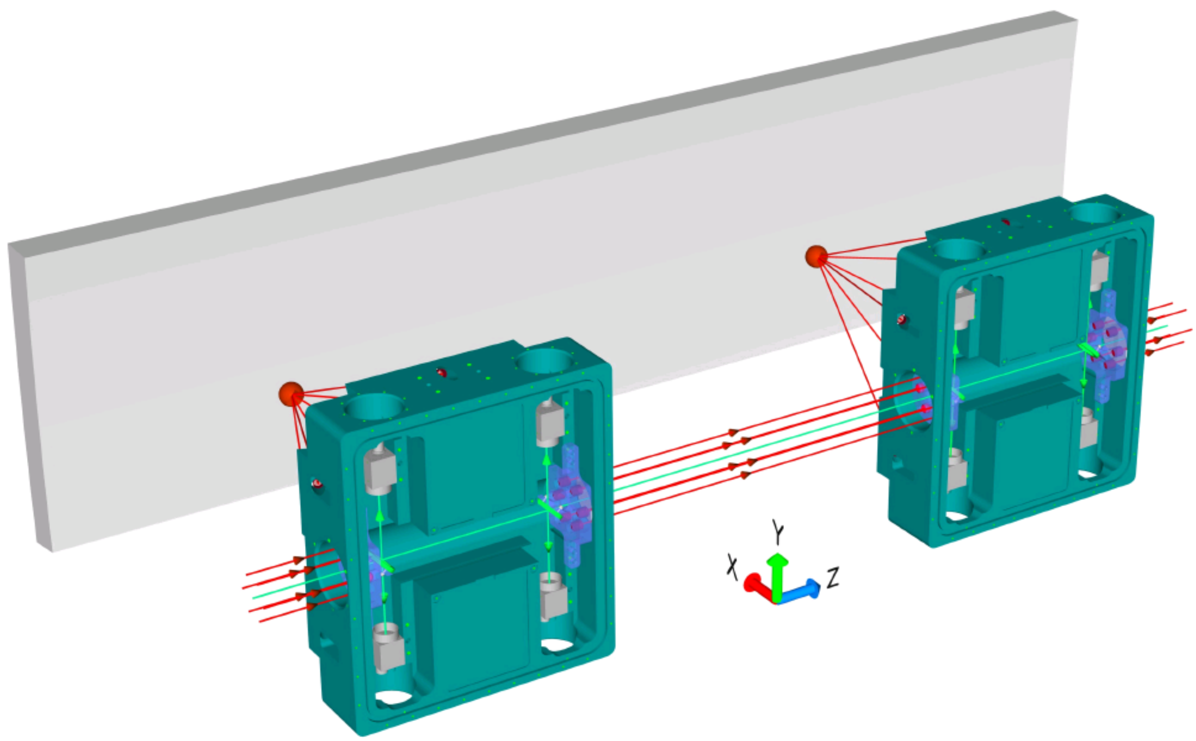


Figure 1: Mechanical design of the measurement units for the LiCAS train. The sensing parts of each car are composed of 4 CCD cameras and 2 beam splitters (BS) constituting the straightness monitor and 6 internal FSI lines to measure the distance between the cars. The 6 external FSI lines pointing towards the tunnel wall measure the position of wall markers.

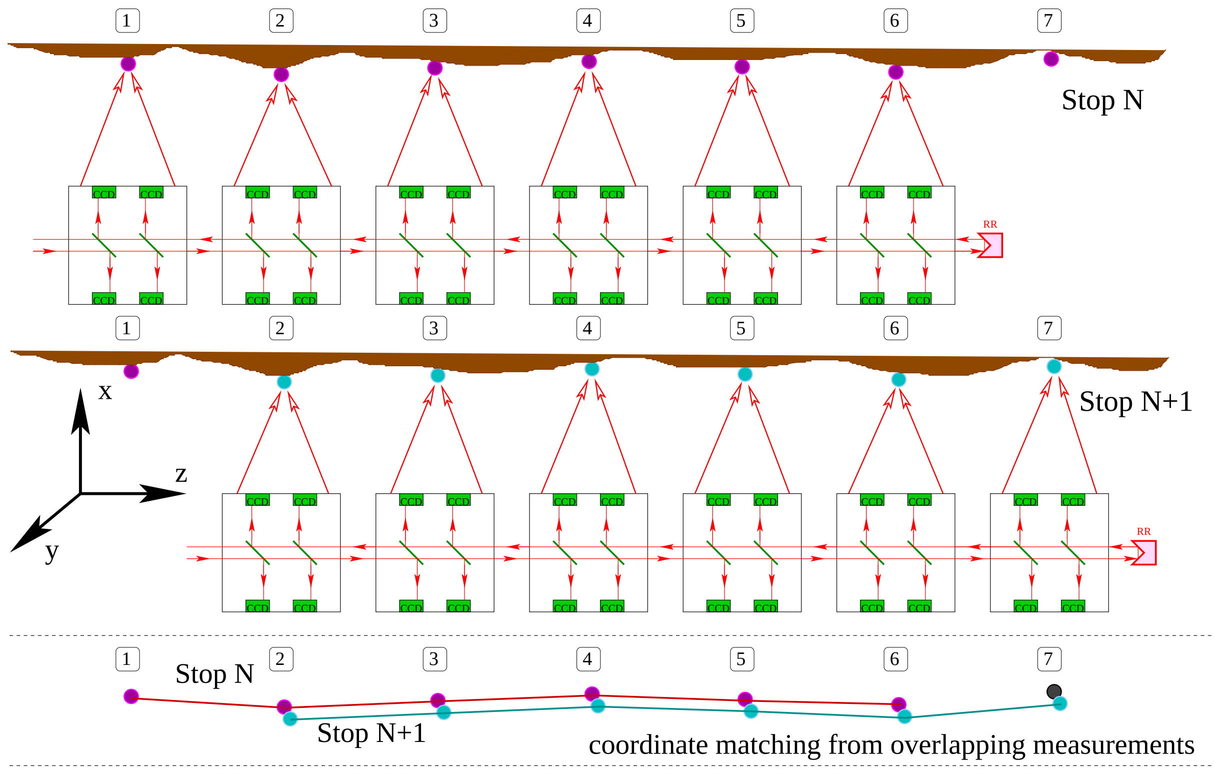


Figure 2: Principle of the LiCAS train operation. Top view of the two train stops along the accelerator tunnel are presented. For detailed description see text.

RTRS follow the geoid along the tunnel length. Geoid variation in $R_z$ along the length of the tunnel have no noticeable influence on the survey procedure.

When the train stops in front of the wall markers it firstly measures the relative position and rotation of all cars with respect to the first car. This defines the local reference frame of the train in which the location of the wall mounted reference markers are measured next. This procedure is repeated for each train stop. Each marker is measured up to 6 times. Finally the coordinates of each marker, expressed in the local train frames are transformed to the frame of the first train (the global frame) by fitting them to each other under the constraint that wall markers have not moved during the entire measurement. Table 1 summarises the degrees of freedom which are accessible for various sensing components of the train.

# 3 OPTO-GEOMETRICAL MODEL OF THE LICAS TRAIN

In order to study the expected precision on the position reconstruction of the tunnel reference markers a simulation of the LiCAS survey train was performed. To describe the sensing parts of the train the SIMULGEO [5] package was used which allows for modelling of the opto-geometrical systems. This software is also capable of performing the full error propagation including correlations between various sub-components linked via common mechanical

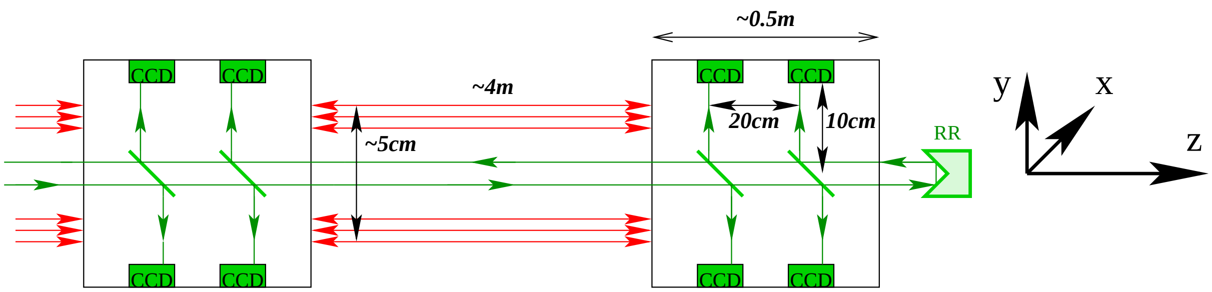


Figure 3: Schematic view of the sensing parts of the LiCAS cars. 4 CCD cameras, 2 beam splitters, 6 internal and 6 external FSI lines and 1 clinometer are located on each car. The first car is equipped with a laser for the straightness monitor and the retro-reflector (RR) is located on the last car.

| Accessible DOF: | | | | | | |
|---|---|---|---|---|---|---|
| | $Tr_x$ | $Tr_y$ | $Tr_z$ | $Rot_x$ | $Rot_y$ | $Rot_z$ |
| LSM | $\surd$ | $\surd$ | | $\surd$ | $\surd$ | |
| INT-FSI | $\pm$ | $\pm$ | $\surd$ | $\pm$ | $\pm$ | |
| Clinometer | | | | $\surd$(not used) | | $\surd$ |

Table 1: Summary of the degrees of freedom measured by various sensing components of the LiCAS train. The FSI measurements marked with $\pm$ have lower sensitivity that the corresponding LSM measurements.

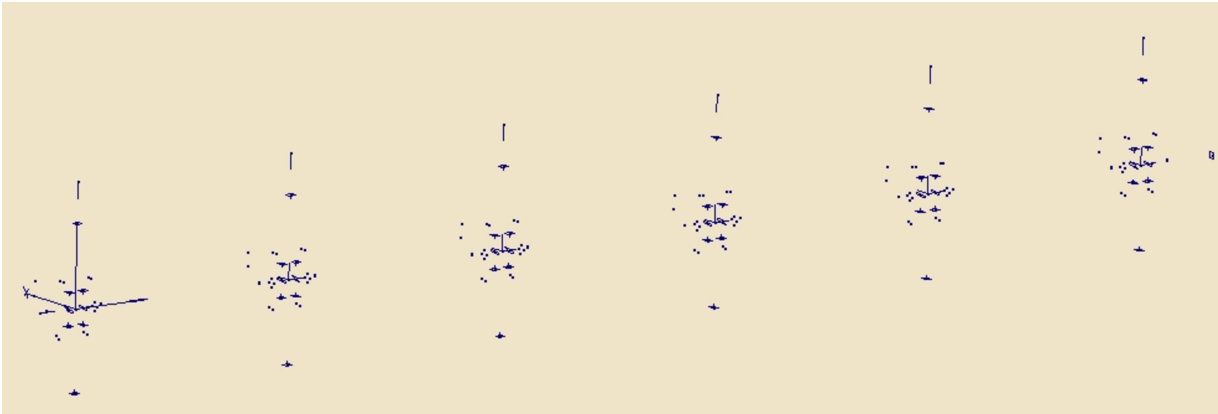

Figure 4: SIMULGEO model of the LiCAS train. 4 CCD cameras, 2 beam splitters, 6 internal and 6 external FSI lines and 1 clinometer are located on each car.

supports.

Within the SIMULGEO framework a train composed of 6 cars was described (fig. 4): Each car was equipped with LSM (4 CCD cameras and 2 beam splitters), 6 internal and 6 external FSI lines and the clinometer (described as a set of 2 CCD cameras sensing a laser beam parallel to the local vertical axis). The first car in the train was also equipped with the laser beam for the LSM. In addition on the last car a second anti-parallel laser beam was located with some offset to account for the beam displacement in the retro-reflector.

This analysis was also very valuable for optimising the LiCAS design. For instance, a weak point of the design was identified to be related to the measurement of the rotation angle around the tunnel axis. Because of the very high ratio of the train length with respect to the transverse dimensions of its vacuum pipe (and to the dimensions of the CCD cameras) this angle cannot be measure with high accuracy using optical methods. To improve the precision of the measurement of this coordinate the application of the clinometers on each car was proposed.

Another example of the design optimisations performed using the SIMULGEO software is the configuration of the straightness monitor (fig. 5). The most intuitive design shown in figure figure 5:1 works well in 2D space but is unable to resolve the ambiguity between translation and rotation around the second transverse axis in 3D space. This problem was solved by adding the retro-reflector which provides a reflected anti-parallel beam (fig. 5:2-4). Configuration no. (4) contains effectively 4 pairs of LSM (each combination of up-down pair of CCD cameras) being the most redundant option selected for the final design.

## 3.1 Simulation of a single train stop

Figure 6 (left column) contains the SIMULGEO results obtained for the simulation of a single train stop. Expected precision on the car positions, car angles and wall markers positions are plotted as a function of car number. The errors on the $z$ position of the cars are growing

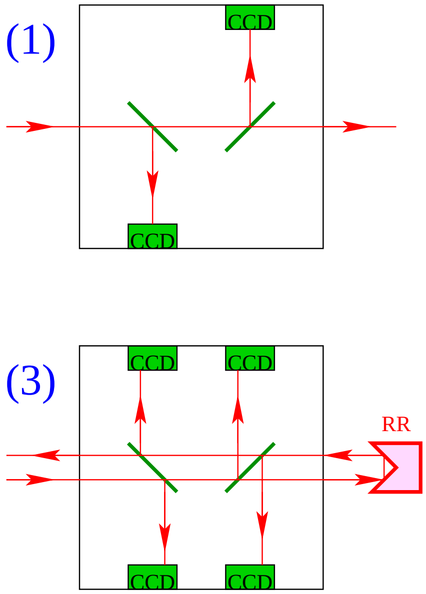


Figure 5: Possible configurations of the laser straightness monitor (LSM): (1) single beam pass version, (2) version with retro-reflector, (3) two LSM in one car, low redundancy (4) two LSM in one car, high redundancy. (RR=retro-reflector).

approximately like $\sim \sqrt{n}$ and the transverse translation errors are constant. This is because the precision of the instruments on all individual cars is identical and the transverse position is measured with respect to the same laser beam which defines the local frame of the train. Car rotation angle around the $z$-axis (tunnel axis) also has constant precision as expected from the independent clinometers located on each car. The above results were obtained assuming the intrinsic resolution of the CCD cameras and FSI lines equal to $\sigma_{CCD} = \sigma_{FSI} = 1\,\mu m$. The assumed precision of the clinometer was $\sigma_{tilt} = 1\,\mu rad$. The reconstruction accuracy of the unknown "walk" of the reflected beam was found to be of the order of $\sigma_{walk} = 0.6\,\mu m$. The above simulation was performed under the assumption that all calibration constants (positions and rotations of CCD cameras, beam splitters, FSI light sources and retro-reflectors) are known to the accuracy of $\sigma_{pos} = 1\,\mu m$ for positions and $\sigma_{ang} = 1\,\mu rad$ for angles. As will be discussed in the section describing the calibration procedure not all of these need to be known to such a high level of precision. Nevertheless the "$1\,\mu m$"/"$1\,\mu rad$" simulations can be regarded as the reference to be compared to results obtained with more realistic values of calibration parameter errors in the future.

### 3.2 Simulation of many overlapping train stops

The long-distance operation of the train inside the accelerator tunnel was simulated by a set of many identical trains displaced by $4.5\,m$ (distance between stops), each pair of them coupled via 5 overlapping wall markers. The results obtained for a distance of $90\,m$ (20 train stops) are presented in figure 6 (right column). The same assumptions as for the single stop

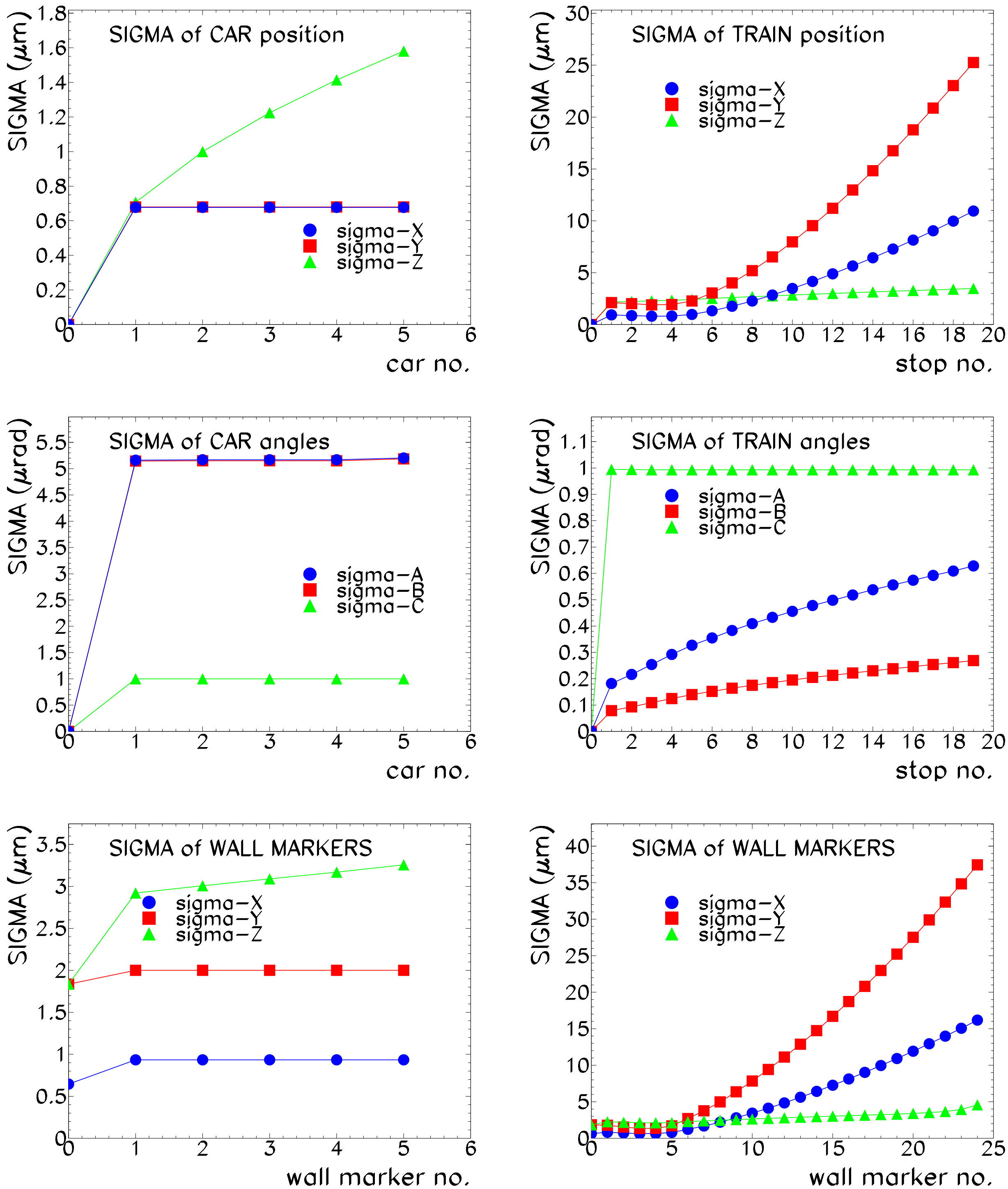


Figure 6: Results of the Simulgeo simulation for the single LiCAS train (left column) and for the 20 stops of overlapping trains (right column). The resolution on $X, Y, Z$ position and rotation angles $A, B, C$ around $x, y, z$ axis for as the function of car or train stop number are plotted. The last row presets the expected precision on the position reconstruction of the wall markers.

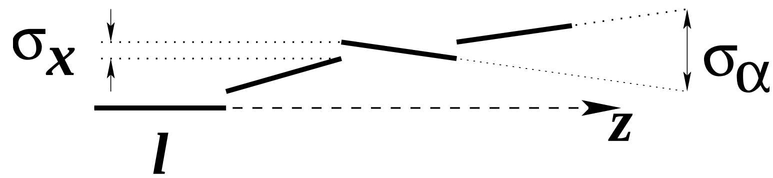


Figure 7: Random walk model for the error propagation for the position of the accelerator components. The overall error is a convolution of the precision of the ruler and the precision of the placement of the ruler with respect to the previous measurement.

simulation were made about the intrinsic precision of CCD cameras, FSI measurements and about the accuracy of the calibration constants.

SIMULGEO calculations provide very precise results based on the exact opto-geometrical model of the survey procedure. However, from the numerical point of view, such an approach, manipulating large matrices, is very time and memory consuming. The 20 stop results were obtained after 34 hours of CPU time using $1\,GB$ RAM memory on a $2\,GHz$ machine (the rank of the used matrix was of the order of 10000). The numerical complexity of these calculations scale like $N^2$, where $N$ is the number of involved coordinates. The simulation of the full $600\,m$ tunnel section would require more then 7 weeks of CPU time.

### 3.3 Random walk model

To overcome the above mentioned limitations a simplified analytical formula inspired by a random walk model was derived to extrapolate the SIMULGEO predictions over long tunnel sections (see also fig. 7):

$$\sigma_{xy,n} = \sqrt{l^2\sigma_\alpha^2\frac{n(n+1)(2n+1)}{6} + \sigma_{xy}^2\frac{n(n+1)}{2}}, \quad \sigma_{z,n} = \sqrt{\sigma_z^2\frac{n(n+1)}{2}} \tag{1}$$

where $n$ is the wall marker number, $l$ is the effective length of the ruler (here: distance between cars), and the corresponding errors are the parameters of the random walk: $\sigma_\alpha$ is the angular error, $\sigma_{xy}$ are the transverse errors and $\sigma_z$ is the longitudinal error.

In this model the procedure of accelerator alignment[3] resembles the construction of a long straight line using short ruler. The overall error is a convolution of the precision of the ruler and the precision of the placement of the ruler with respect to the previous measurement. The asymptotic behaviour of the formulae from equation no. 1 is:

$$\sigma_{xy,n} \sim n^{\frac{3}{2}}, \quad \sigma_{z,n} \sim n. \tag{2}$$

This fast growth of errors (especially for transverse directions) is a consequence of the fact that the errors are highly correlated and the precision of the $n^{th}$ element depends on the precision of all previous points.

[3]We assume here that the precision of the accelerator alignment will be similar to the precision of the reference marker measurement as wall markers are located close to all accelerator components.

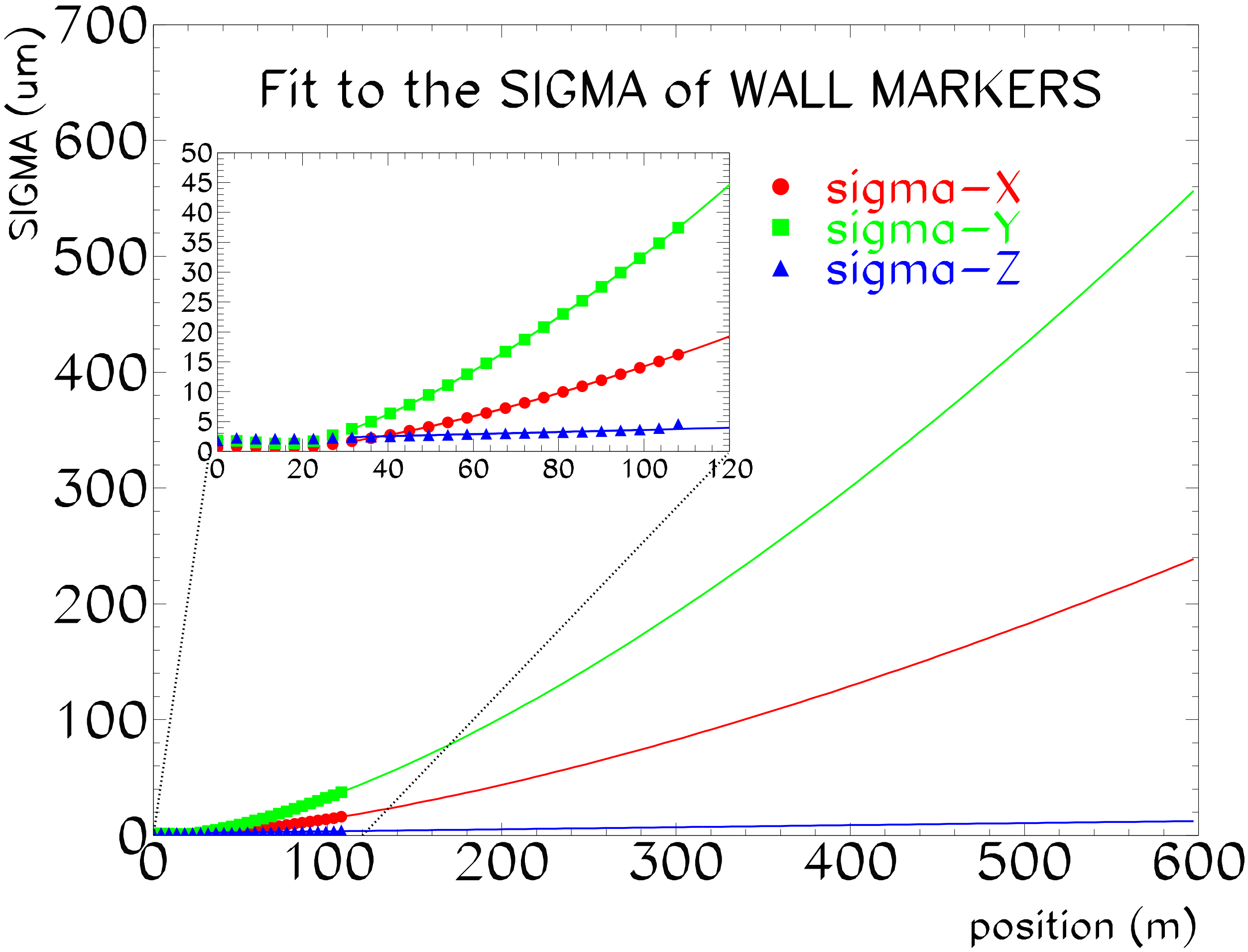


Figure 8: The LiCAS train simulation: insertion contains the results of the exact simulation obtained with the Simulgeo, extrapolated on the main plot to the $600\,m$ tunnel section using the formula from the random walk model.

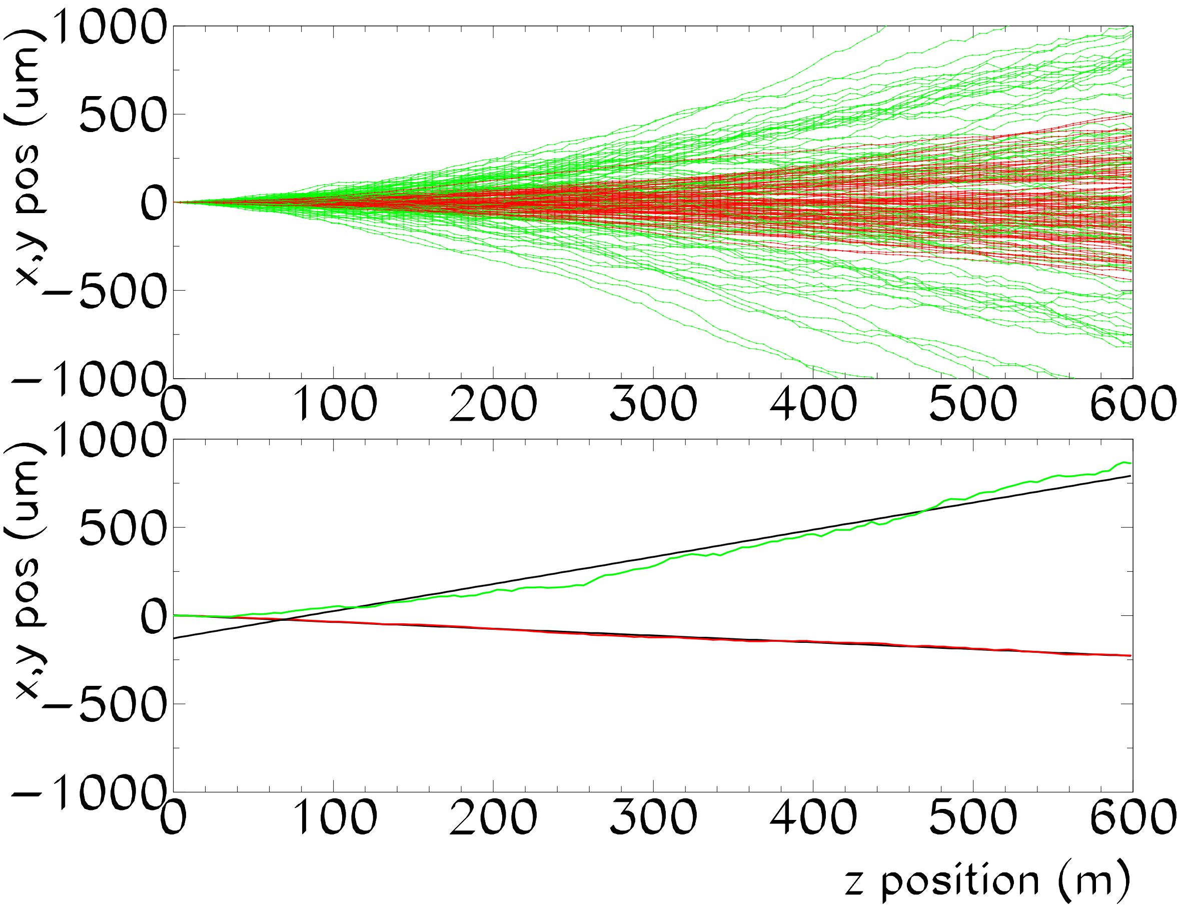


Figure 9: Examples of the random walk trajectories (upper plot) and straight line fits to two selected trajectories (lower plot).

Formulae 1 were fitted to the Simulgeo points determining $\sigma_\alpha$, $\sigma_{xy}$, $\sigma_z$ and then extrapolated over a $600\,m$ tunnel section (fig. 8). The obtained predictions refer to the precision of the placement of the $n^{th}$ accelerator component with respect to the first one. However this is not the ultimate measure of the quality of the accelerator alignment. The relevant parameter is the mean deviation of each component from the ideal straight line which can be expected from the above procedure.

To obtain the final prediction on the deviation of the alignment from the straight line a series of random walk trajectories was generated using the parameters fitted to the Simulgeo points (fig. 9). A straight line was fitted to each trajectory and the corresponding residua were calculated. The extracted RMS values of the residua distribution provide the measure of the accuracy of the whole procedure. Because of high correlation between errors for $n$ and $n+1$ marker the generated trajectories exhibit much smaller oscillations that would be expected from completely random process. Figure 10 summarises the results obtained in

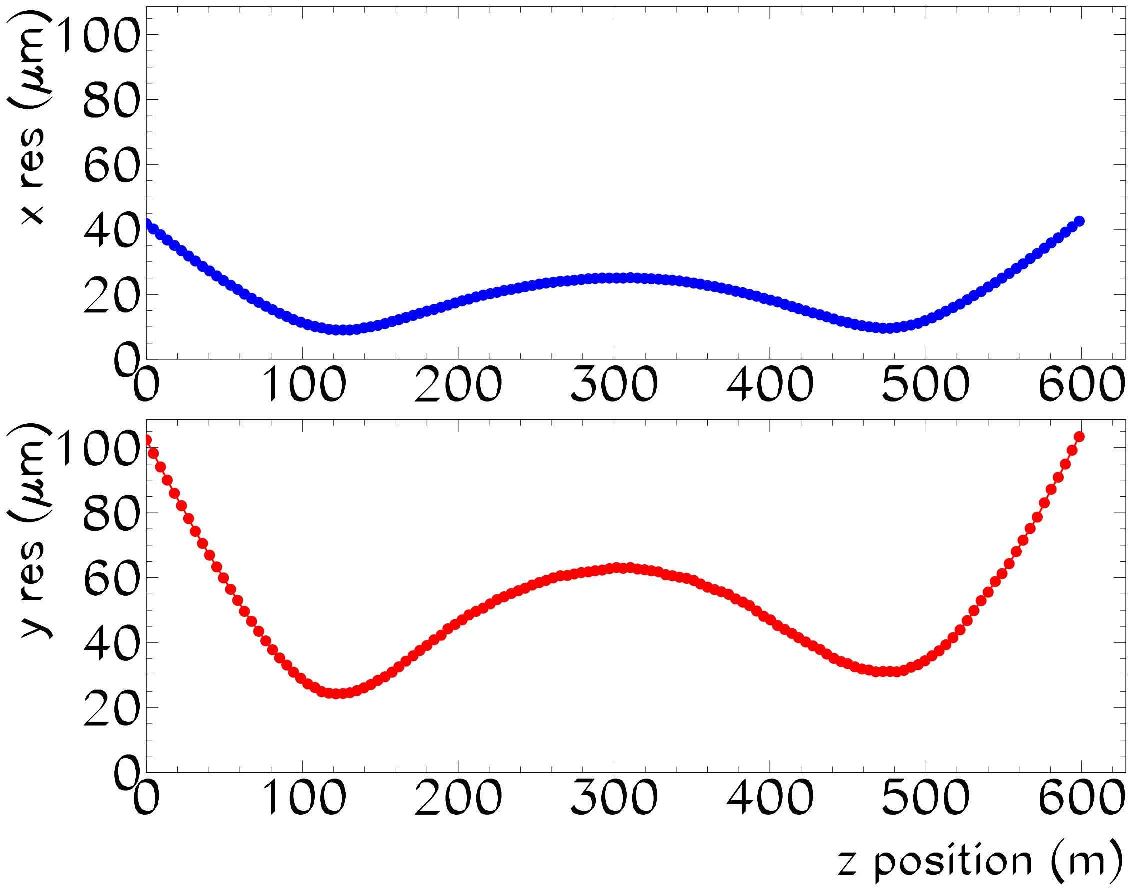


Figure 10: RMS of the residua distribution from the straight line fit to the random walk trajectories: horizontal (upper plot) and vertical direction (lower plot).

this analysis demonstrating that the vertical precision of the order of $\mathcal{O}(100\,\mu m)$ over $600\,m$ is feasible.

## 4 CALIBRATION OF THE LASER STRAIGHTNESS MONITOR

The precise knowledge of the positions and rotation angles of the "active" car components will be crucial for proper determination of the wall marker positions. A first attempt has been made to develop a calibration procedure for the straightness monitor. The principle of this procedure is based on a multi-dimensional parameter scan. The straightness monitor is located on motion stages which provide accurate translational and rotational motion in the 4 DOF to which the LSM is sensitive[6].

During the scans the whole straightness monitor can be treated as a rigid body in which the relative positions of the CCD cameras and beam splitters remain unchanged. A suffi-

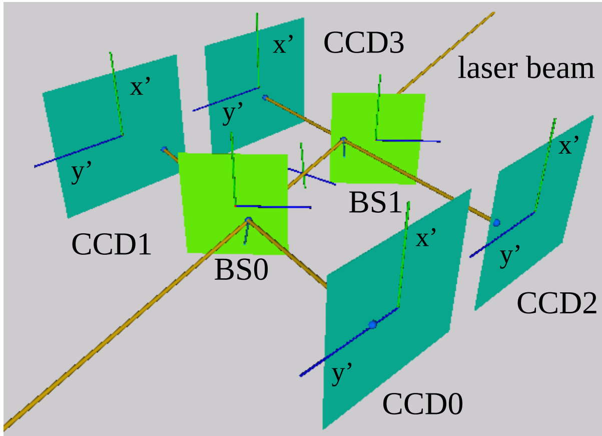


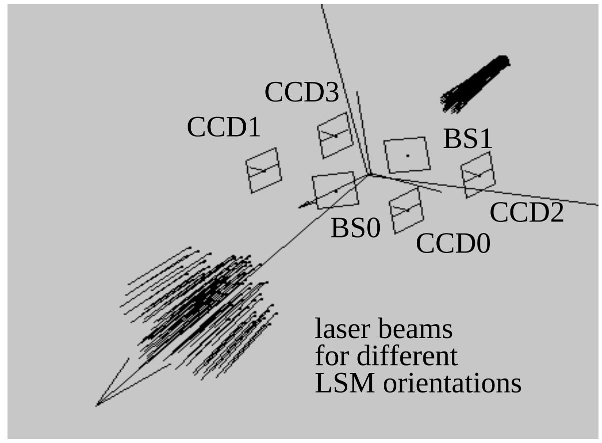


Figure 11: Calibration of the Laser Straightness Monitor. Left picture illustrates ray tracing simulation producing data for the SIMULGEO reconstruction (right). The bundle of lines on the right plot represents the different positions and orientations of the laser light source with respect to the LSM as used in the multi-dimensional parameter scan.

ciently large set of measurements from the CCD cameras will allow reconstruction of the unknown calibration constants via a heavily over-constrained fit. The minimised function is a ray tracing model of the LSM parametrised by the calibration constants and the optimal solution is the one for which all the CCD measurements can be consistently reproduced by the ray tracing algorithm.

To proof this calibration principle a simulation was written where a set of "artificial data" obtained from a ray tracing program was used as an input for SIMULGEO (fig. 11). The precision of the motion stage was assumed to be $\sigma_{x,y} = 0.05\,\mu m$ and $\sigma_{A,B} = 1.7\,\mu rad$ for translation and rotation ($A = R_x$, $B = R_y$), respectively. CCD camera no. 0 (fig. 12) was chosen to define the local coordinate frame of the car (i.e. its position was assumed to be exactly known and all other coordinates were expressed in its frame). The obtained calibration constants were of the order of: $\sigma^{BS}_{ang} = 5\,\mu rad$ for beam splitter rotation angles and $\sigma^{CCD}_{pos} = 4\,\mu rad$ for the position of the CCD cameras. The lowest absolute sensitivity was found for determining the angles of the CCD cameras: $\sigma_{A,B} = 70\,\mu rad$ and $\sigma_C = 10\,\mu rad$ ($C = R_z$). However the transverse size of the CCD camera is of the order of $1\,cm$ and the cameras are displaced by only $10\,cm$ from the beam splitters. Such an angular uncertainty will therefore be translated into sub-micron motion on the beam-spot position on the surface of the CCD camera. A full SIMULGEO simulation with random walk extrapolation to $600\,m$ using the above calibration constants provides predictions on the accuracy of the tunnel survey only by 10% worse that the numbers presented in figure 8.

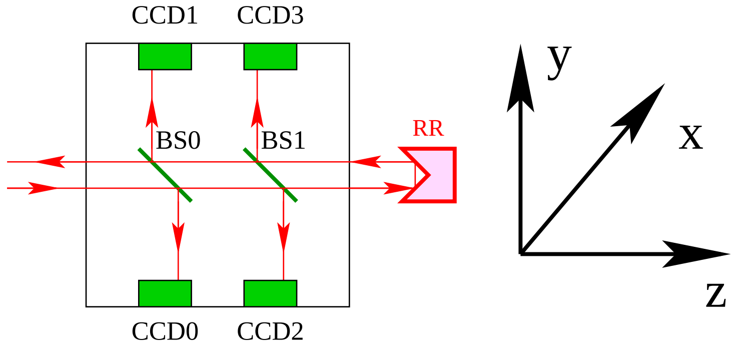


Figure 12: Straightness Monitor configuration used for the test of the calibration procedure. CCD0 defines the local reference frame of the car.

## 5 CONCLUSIONS

Full SIMULGEO simulations of the LiCAS train were performed for a $90\,m$ tunnel section. The predictions were extrapolated to $600\,m$ using a random walk Monte Carlo model. The results obtained for the precision of the linear collider alignment are well below the specifications for TESLA which are of the order of $\mathcal{O}(200)\,\mu m$ over $600\,m$ for the vertical co-ordinate. A first successful attempt to design a calibration procedure for the LiCAS train was also presented.

# References

[1] P.A. Coe, D. F. Howell and R. B. Nickerson “Frequency scanning interferometry in ATLAS: remote, multiple, simultaneous and precise distance measurements in a hostile environment”, Meas. Sci. Technol. 15 (2004) 2175-2187.

[2] A.F. Fox-Murphy et al., “Frequency scanned interferometry (FSI): the basis of the survey system for ATLAS using fast automated remote interferometry”, Nuclear Instruments and Methods in Physics Research A 383 (1996) 229-237.

[3] M. Schlösser, “The Rapid Tunnel Reference Surveyor for a future linear collider”, IWAA2004, published in this Volume.

[4] “TESLA, The Superconducting Electron-Positron Linear Collider with an Integrated X-Ray Laser Laboratory”, Technical Design Report, DESY 2001-011.

[5] L. Brunel, “SIMULGEO: Simulation and reconstruction software for optogeometrical systems”, CERN CMS Note 1998/079.

[6] A. Mitra et al. “Measurements of the LiCAS systems”, IWAA2004, published in this Volume.